

## Thermal Conductivity and Connectivity in Polycrystalline MgB<sub>2</sub>

E.A. Young, A. Kulak, .Y. Yang

*School of Engineering Sciences, University of Southampton, SO17 1BJ*

In polycrystalline superconductor MgB<sub>2</sub> only a fraction of cross section carries electrical current, which as has been previously shown can be worked-out from the normal state electrical resistivity. For the first time we apply the electrical cross section to the thermal conductivity of 6 polycrystalline samples with grain sizes from 20nm to 4 $\mu$ m. The calculated thermal conductivity of 5 out of the 6 samples with a large effective area fraction (>0.3), converge at T>300K. By modeling with an electronic transport of heat the same thermal lattice properties are obtained for the 5 samples from the temperature dependent thermal resistivity from 40K to 100K.

There has been much recent reference to a proposal that high normal state resistivity in many MgB<sub>2</sub> samples can be explained by a reduced electrical cross section<sup>1,2,3</sup>. A method was suggested to extract an effective cross section from the 40 to 300K normal state resistivity data by comparison with the temperature dependent resistivity  $\Delta\rho(T)$  of a known reference sample<sup>4</sup>. The method has also the advantage that a more correct residual resistivity  $\rho(0)$  can be calculated to give some information on the degree of electron scattering. To date the method has been used as a tool to qualify the cross section of the current in the superconducting state, and aid materials investigations to optimise the microstructure for current transport. However as Rowell<sup>4</sup> discussed, due to inclusions of oxides and impurities in many samples there are many possible resistive effects, perhaps at grain boundaries, which are not easily separable from the grain properties. For the first time expand Rowell's method to apply the electrical effective cross section to the thermal conductivity.

The most recent measurements on single crystals, show the normal state has an essentially electronic thermal conduction. As the Debye temperature, (890K)<sup>5</sup>, is approached the thermal conductivity of the same chemical lattice will approach the same value, regardless of microstructure defects, which is a consequence of the 1/temperature dependence of the residual thermal resistance. In contrast the residual electrical resistivity is a constant value and is still significant at 300K so no convergence is expected. Using the resistivity data to remove the effect of porosity, it can be seen if the in the thermal conductivity of polycrystalline samples is commensurate in the high temperature range.

6 samples are investigated, 3 made in house, and in order to extend the investigation to larger grain sizes, 3 samples from the literature<sup>6</sup>. In-house samples were prepared from <1 $\mu$ m, high purity 99.9% boron, packed into a Ta (99.9%) lined Fe

(98%) crucible, to 40% dense, a Mg rod, 99.9%, packed on top, and a vacuum applied before welding shut. To vary the grain size three samples were produced using different heat treatments. Sample 1, 750°C for 10 hours, sample 2 850°C for 10 hours, and sample 3 1000°C for 1 hour, 930°C for 3 hours, 800°C for 10 hours. The bulk samples turned out of the crucibles in a lathe, are very reactive to air and water, yet no degradation within 1 year has been measured, showing surface oxidation protects the bulk from degradation. Samples were diamond cut and polished to bars 12mm long, with a square cross section of 0.5 to 1mm<sup>2</sup>. The largest error of 10% comes from the finite size of the contacts. Resistivity and thermal conductivity were measured on the same section of sample in a Quantum Design PPMS.

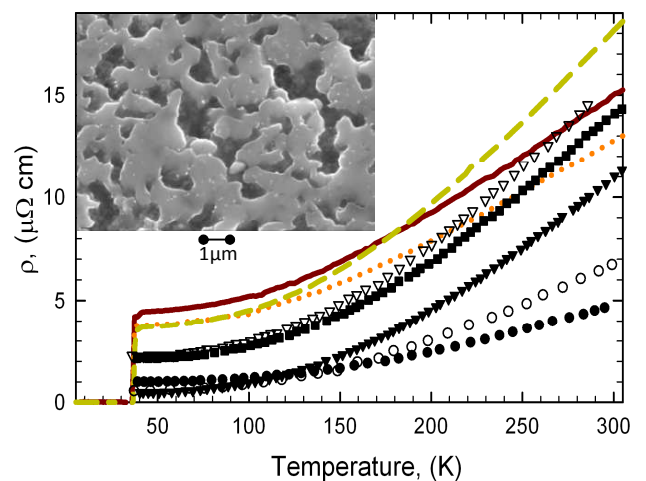


FIG. 3. (Color online) Resistivity of polycrystalline samples, in house plotted as lines, samples 1(solid), 2 (dotted), 3 (dashed), from Putti<sup>6</sup> open symbols 4, (circle), 5, (triangle). Reference samples are filled symbols, SC Lee, (circle), CVD wire Ribeiro, (square), SC Sologubenko (triangle). Inset is an electron

TABLE 1. Extracted properties of MgB<sub>2</sub> polycrystalline samples.

Sample		$\rho(40K)$ ( $\mu\Omega$ cm)	F	$A_F$	$\rho(0)$ ( $\mu\Omega$ cm)	$\beta$	$L_0$ (from $\beta$ )
1	In-situ 750°C	4.55	2.5	0.40	1.8	0.64	2.81
2	In-situ 850°C	3.78	2.1	0.48	1.8	0.64	2.81
3	In-situ 950°C	3.68	3.4	0.29	1.1	0.37	2.97
4	In-situ 11-1S	0.55	1.4	0.71	0.4	0.14	2.86
5	In-situ 1S	2.29	3.2	0.32	0.7	0.23	3.04
6	Ex-situ TS	43.2	24.0	0.09	1.8	--	--

The MgB<sub>2</sub> microstructure seen for sample 3 inset Fig. 1 is well suited to a first connectivity study, there are pores, but no obvious oxides or cracks and grain boundaries are well formed. There is however quite a large variation in grain size, from 300nm to 4  $\mu$ m. Samples 1 and 2, which are not shown also have a range of grain sizes from 20nm to 500nm. The as measured resistivity presented in Fig. 1, vary by up to a factor of 3 at 300K. The  $\rho(40K)$  are close to temperature independent behaviour and is taken to be the residual resistivity, (presented in Table 1.). The resistivity of sample 6 is a factor of 10 too large for the scale in Fig.1, and although no further investigation of this sample will be presented it is worth including only to highlight the current difference between the much poorer connectivity of ex-situ reacted MgB<sub>2</sub> and in-situ reacted.

Consistent with Rowell<sup>4</sup> the effective fraction of cross section ( $A_F=1/F$ ) is calculated from the resistivity. Rowell used the lowest published value of  $\Delta\rho^{SC}$  for single crystals, of 4.3  $\mu\Omega$ cm<sup>7</sup>, but later authors have used 7.3  $\mu\Omega$ cm from the most ideal polycrystalline material<sup>8</sup>. The resistivity of these two reference samples plus single crystal data from Sologubenko<sup>9</sup> - included as they are the only published measurement of thermal conductivity on single crystals - are plotted in Fig. 1. The difference in resistivity between the displayed reference samples varies by a factor of 3, which leaves uncertainty over what constitutes the ideal sample. To examine any further fundamental difference in the presented reference samples,  $\Delta\rho^{SC}(T)$  extracted from the publications, was scaled to the smallest value from Lee, and it was found that the temperature dependence of all 3 reference samples was identical. The difference in resistivity between the reference samples can then be described solely by  $\Delta\rho^{SC}$  and  $\rho(0)$  and a factor such as F in equation 1, which suggests that the most likely explanation for the difference between these reference samples is dimensional, if this is not the case then another interpretation of F and Rowell's published method would be required.

For the purposes of this study the only requirement for the reference is that  $\Delta\rho^{SC}$  has to be smaller than the  $\Delta\rho^{SC}$  of the

polycrystalline samples, otherwise  $F < 1$ . For this reason only the  $\Delta\rho^{SC}$  of Lee's reference sample is used as it is the only reference sample that meets this requirement.

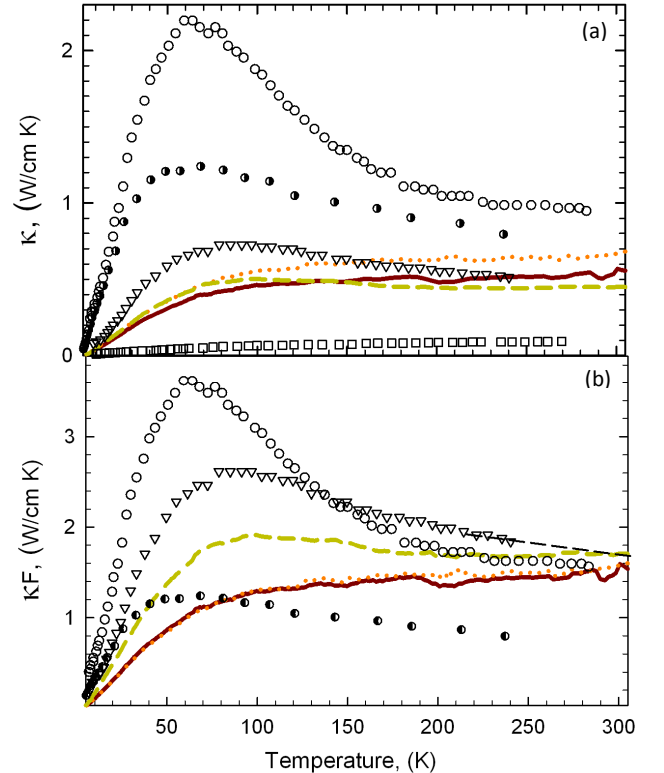


FIG. 2. (Color online) Thermal conductivity as measured, (top); divided by the effective cross section F, (bottom) . Lines are samples 1(solid), 2 (dotted), 3 (dashed ), symbols from Putti<sup>6</sup> open symbols 4, (circle), 5, (triangle), 6(square). Half filled circle single crystal<sup>9</sup>. The dashed line extrapolates sample 5 to 300K.

The results for the connectivity factor F for the polycrystalline samples presented in Table 1 show F to be between 1.4 and 3.4 for 5 of the samples and 24 for sample 6. The  $\rho(0)$  of 0.4  $\mu\Omega$ cm and 0.8  $\mu\Omega$ cm for samples 4 and 5 are lower than the reference sample value of 1.0  $\mu\Omega$ cm, which would mean the polycrystalline samples are purer than the single crystal. It is unusual for polycrystalline samples to have a higher purity than

single crystals, but there is a precedent, as seen in Fig. 1. for Ribeiro's CVD wire sample which has a lower  $\rho(40\text{K})$  than the single crystals.

The thermal conductivity of samples 1 to 6 are presented in Fig.2.(a) The values vary from 0.1 to 1 W/cm K at 300K, the lowest value is the ex-situ sample, 6. The largest grained sample, 3, (from 1 to 4 $\mu\text{m}$ ) has the highest thermal conductivity at low temperatures, 70K, which is expected for samples with more annealed larger grains, as there is less defect scattering, but  $\kappa(300\text{K})$  is also higher than all the samples, which is not expected in this temperature range where the scattering is from the  $\text{MgB}_2$  lattice. Sample 3 also has a higher thermal conductivity than the single crystal, not only at 300K, but the increase from  $\kappa(300\text{K})$  to the  $\kappa(70\text{K})$  peak, is more, so cannot be explained by dimensional arguments alone, but would require the single crystal to have more electron scattering, which again could be due to a lower purity.

We calculate the thermal conductivity by multiplying the effective area with the measured thermal conductivity, (plotted (Fig 2.(b)). The result shows that all the extracted thermal conductivity data converge to a small range of values at 300K, between 1.4 and 1.6 W/cm K. Although 300K is less than half the Debye, the measured temperature dependence of  $\kappa$  is very small and notwithstanding anomalous behaviour should not change a great deal at higher temperatures – further work of  $\kappa$  measured to higher temperatures would confirm this.

At lower temperatures the thermal conductivity separates due to electron scattering. In Fig. 3 is a plot of  $WT$  vs  $T^3$ , where the thermal resistance  $W=1/\kappa$ , and the result is a straight line with intercept  $\beta$  and slope  $\alpha$ , which fits electronic heat conduction. The only data which does not fit this electronic model of heat conduction is the single crystal which is in contradiction with the conclusions presented and cannot easily be explained by dimensional arguments. The intercept  $\beta$  from the fitting curve is linked to  $\rho(0)$  according to the Wiedemann-Franz law. By inserting  $\rho(0)$  from the resistivity measurements we achieve values of  $L_0$  within 20% of the theoretical Lorentz constant,  $2.45 \times 10^{-8} \text{V}^2/\text{K}^2$ , (see Table 1). At 300K taking the resistivity of the reference as  $5.3 \mu\Omega \text{ cm}$ , and  $\kappa=1.5 \text{W/cm K}$ ,  $L_0=2.65 \times 10^{-8} \text{V}^2/\text{K}^2$ , again all samples within 20% of theoretical. The residual thermal resistance depends on  $\beta$ , and it is interesting to see in Table 1, there is a roughly linear correlation with grain size – rough due to the large variation in grain sizes in any one sample. As  $\beta$  scales with grain size then it may be that the electron scattering is predominantly at grain boundaries, which would have implications for the materials processing and optimisation of current transport properties.

By applying a connectivity model using the electrical resistivity to the thermal conductivity it has been shown how the thermal

lattice properties of different  $\text{MgB}_2$  bulk samples can be calculated after accounting for porosity. The convergence of the calculated thermal conductivity at 300K, and the equivalence of the temperature dependent thermal conductivity constant  $\alpha=2.4 \times 10^{-7} \text{ m}^2/\text{W K}$  40K to 100K, demonstrate that for these samples the connectivity model satisfactorily accounts for the porous microstructure. There is however still some controversy over the choice of reference sample which will affect the final result.

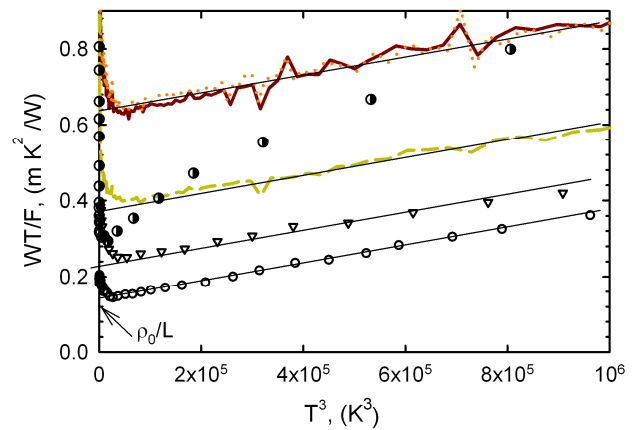


FIG. 3. (Color online) Thermal resistance of polycrystalline samples, in house plotted as lines, samples 1(solid), 2 (dotted), 3 (dashed ), from Putti<sup>3</sup> open symbols 4, (circle), 5, (triangle). Single crystal Sologubenko (half filled circles). Straight black lines are a fit to  $WT=\alpha T^3+\beta$ , with  $\alpha=2.4 \times 10^{-7} \text{ m}^2/\text{W K}$ .

## References

- <sup>1</sup>X. Xu, J. H. Kim, S. X. Dou, S. Choi, J. H. Lee, H. W. Park, M. Rindfleisch, M. Tomsic, J. Appl. Phys., 105, 103913 (2009).
- <sup>2</sup>J. Jiang, B.J. Senkowicz, D.C. Larbalestier, E. E. Hellstrom, Supercond. Sci. Technol. 19 (2006) L33–L36.
- <sup>3</sup>A. Malagoli, V. Braccini, M. Tropeano, M. Vignolo, C. Bernini, C. Fanciulli, G. Romano, M. Putti, C. Ferdeghini, E. Mossang, A. Polyanskii, D. C. Larbalestier, J. Appl. Phys. 104, 103908 (2008).
- <sup>4</sup>J.M. Rowell, Supercond. Sci. Technol. 16 (2003) R17–R27.
- <sup>5</sup>T. Masui, K. Yoshida, S. Lee, A. Yamamoto, S. Tajima, Phys. Rev. B, 65, 214513.
- <sup>6</sup>M. Putti, V. Braccini, E. Galleani, F. Napoli, I. Pallecchi, A.S. Siri, P. Manfrinetti, A. Palenzona, Supercond. Sci. Technol. 16 (2003) 188–192.
- <sup>7</sup>Yu. Eltsev, S. Lee, K. Nakao, N. Chikumoto, S. Tajima, N. Koshizuka, and M. Murakami, Phys. Rev. B, 65, 140501(R).
- <sup>8</sup>R.A. Ribeiro, S.L. Budko, C. Petrovic, P.C. Canfield, Physica C 382 (2002) 194–202.
- <sup>9</sup>A. V. Sologubenko, N. D. Zhigadlo, J. Karpinski, and H. R. Ott, Phys. Rev. B, 74, 184523, (2006).